SciTech Publishing
an imprint of the IET

STIMSON'S

# Introduction to Airborne Radar

Third Edition

George W. Stimson
Hugh D. Griffiths
Chris J. Baker
Dave Adamy

STIMSON'S

# Introduction to Airborne Radar

Third Edition



George W. Stimson
Hugh D. Griffiths
Chris J. Baker
Dave Adamy

SciTech Publishing
an imprint of the IET

Editor: Dudley R. Kay
10 9 8 7 6 5 4 3 2 1

# Contents

## PART IX Special Topics and Advanced Concepts

# 16

# Pulse Compression and High-Resolution Radar


*Original cavity magnetron, 1940*



Ideally, to obtain both long detection range and fine range resolution, extremely narrow pulses (for fine resolution) of exceptionally high peak power (for long range) should be transmitted. However, there is a practical limit on the amount of peak power that subsequently limits the detection range. This peak power limit forces the use of long pulses at the expense of range resolution.

The solution to this dilemma is pulse compression, in which coding is modulated onto long, peak power–constrained pulses during transmit, followed by "compression" of the received echoes by decoding their modulation. This provides the necessary average power for an achievable level of peak power. This chapter introduces the fundamental principles of pulse compression and the various classes of modulation coding, otherwise known as the radar *waveform*.

## 16.1 Pulse Compression: A Beneficial Complication

Pulse compression might appear to be an unnecessary complication to the notion of how radar operates. Narrow pulses can easily provide the desired range resolution by setting the pulse width. For relatively short-range operation this arrangement is acceptable. However, if one wishes to have long-range detection capability, it becomes clear from the radar range equation (see Chapter 13) that increasingly high peak powers are necessary. However, there are practical limits to what can be made available from a realistic radar transmitter. The necessary extension to longer pulses subsequently establishes a set of trade-offs to design the appropriate transmitted signal and


**Figure 16-1.** With a short pulse, closely spaced targets can be resolved. However, the limit on peak power likewise limits the maximum detectable range.


**Figure 16-2.** With the increased energy from a long pulse, the maximum detection range can be extended. Pulse compression is now required to separate the closely spaced targets.

receive filtering to perform the desired radar sensing function. It is also worth noting that echo-locating mammals seemed to have developed this capability long before radar engineers ever thought of it.

***The Pulse Width Dilemma.*** Figure 16-1 illustrates an example of the transmission of a short pulse (at peak power) and the resulting echoes from two targets that are closely spaced in range. As long as these targets are separated by more than the pulse width it is possible to distinguish one from the other. However, because there is a limit to the amount of peak power the transmitter can achieve, this short pulse approach severely limits the maximum range from which targets can be reliably detected.

To extend the maximum detection range, more energy is required to be "put on the target." Since the peak power is bounded, the pulse width must be increased (in time). Figure 16-2 shows an example of what occurs when the short pulse from Figure 16-1 is extended in time (pulse width) by a factor of 5. The energy that is incident onto, and thereby reflected from, a target also increases by a factor of 5, thus extending the maximum detection range. However, now there is overlap between the two closely spaced targets such that they cannot be distinguished from one another. The solution to this problem is pulse compression.

***Waveforms.*** In radar, the waveform is simply the transmitted signal. This may be a continuous signal or it may be a pulse. The notion of a radar waveform is extended here to include a modulation imparted upon a pulse. In principle, this modulation could be in terms of frequency/phase, amplitude, or polarization, though the former is by far the most common. Taken as a whole, pulse compression involves the transmission of a modulated, pulsed waveform followed by filtering of the received echoes, where the filter is coherently matched to the waveform.

There are often numerous objectives to be considered when designing a waveform, including

- Total energy of the modulated pulse (this relates to the SNR of received echoes)
- Discrimination between delay-shifted versions of the waveform (for both range resolution and sensitivity)
- Impact of Doppler shift
- Low probability of intercept (by a potential adversary)

The pulse energy is maximized when the amplitude envelope of the pulse is constant. The delay and Doppler characteristics of a waveform are collectively referred to as the waveform *ambiguity function* (see Chapter 11). The intercept probability of a waveform is dependent upon whether it appears to be man-made or naturally occurring (noise radar is an example of the latter).

Most commonly, a waveform can be ascribed to one of the following classes: frequency modulated chirp (linear or nonlinear) or phase-coded waveform (biphase or polyphase).

Linear frequency modulation (LFM) chirp is the most widely used of all waveforms due to its simplicity of implementation on transmit, its robustness to Doppler shift, and the existence of a useful wideband receiver filtering structure known as *stretch processing*. However, due to relatively high time-delay (range) sidelobes resulting from LFM matched filtering, nonlinear frequency modulation (NLFM) and phase-coded waveforms have been devised as possible alternatives.

***The Matched Filter.*** What actually happens when an echo passes through a filter that is matched to the transmitted waveform can be visualized if the echo is thought of as consisting of a sequence of subpulses, or *chips*, each with a distinct phase. As depicted in Figure 16-3 the matched filter is likewise a sequence of chips, though each possesses the conjugate phase (i.e., reflected about the real, or horizontal, axis). If the aligned sets of chips are piecewise multiplied, they all produce the same value (here, set to an arbitrary phase of $e^{j0} = 1$ for simplicity) such that they add constructively in phase.

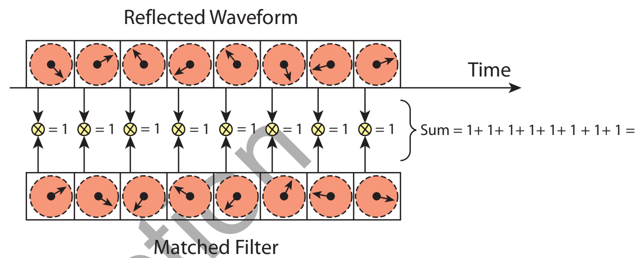


**Figure 16-3.** For a waveform represented as a sequence of 8 chips, the matched filter constructively combines the segments to yield a processing gain, also known as the *pulse compression ratio*, of 8.

Figure 16-3 depicts the precise point in time when an echo aligns with the matched filter, thus producing a gain on the echo. At other delay shifts a different phenomenon is observed. For example, Figure 16-4 illustrates what occurs when the echo is shifted in time by just one chip interval compared with the matched case of Figure 16-3. This time, when the aligned chips are piecewise multiplied, a set of phase values is produced that are out of phase with each other and thus combine destructively when added. The resulting summation will typically be much smaller than the matched case of Figure 16-3. For other delays, different sets of phases are produced by the matched filter, which subsequently yields different destructive combinations that vary as a function of delay in a way that is characteristic to each individual waveform.

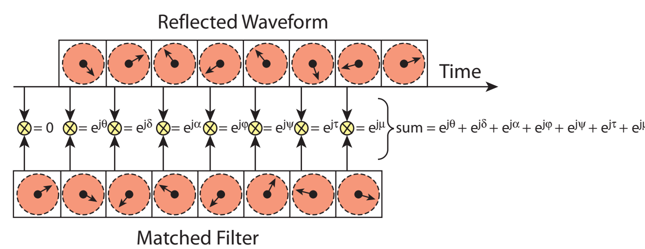


**Figure 16-4.** For delays different from the match point, the segments of the echo do not match the phase sequence of the matched filter, thereby combining destructively to produce a smaller value (here, much less than 8).

In reality, a physical waveform must be continuous. For the discrete illustrations in Figures 16-3 and 16-4 the chips can be thought of as representing basic phase shapes that enable the adjacent chips to connect in a continuous manner over the extent of the waveform (and likewise the matched filter). When considered in this way, the matched filter concept extends to all types of frequency modulated and phase-coded waveforms.

It is becoming increasingly common to perform matched filtering digitally, thus requiring sampling of the received echoes and a digital representation of the filter. The determination of the sampling rate involves a trade-off between higher computational complexity and the acceptable degree of loss from *range straddling* (also known as *range cusping*) that occurs when an echo is not sampled precisely at its matched position.

The continuum of delay shifts comprising the matched filter response to a single echo (with no Doppler) is actually the

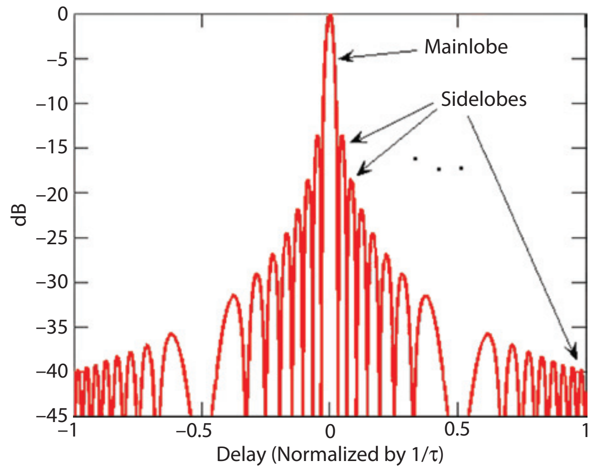


**Figure 16-5.** The matched filter response (waveform autocorrelation) for an LFM chirp with uncompressed pulse width τ illustrates the mainlobe and sidelobes in delay that would result from a single target echo.

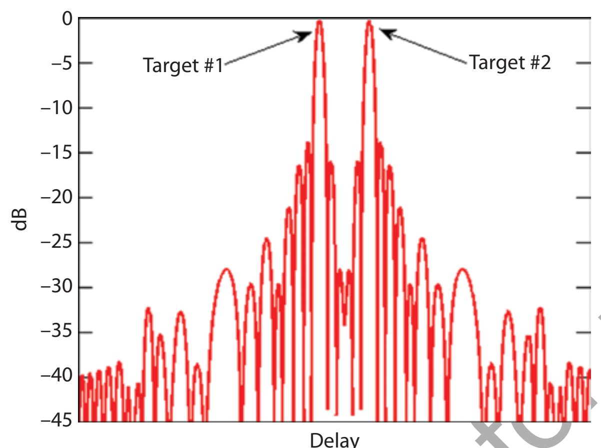


**Figure 16-6.** The echoes from two closely spaced targets may be resolved if they have similar receive powers and are not too close together.

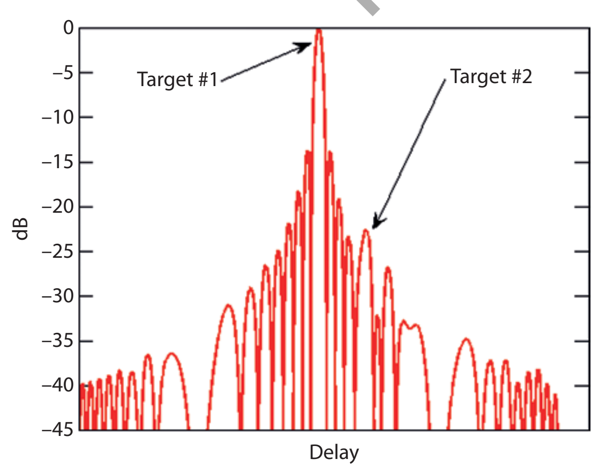


**Figure 16-7.** If the receive echoes from two closely spaced targets have sufficiently disparate receive powers, then the smaller target may be lost among the range sidelobes of the larger target.

autocorrelation of the transmitted waveform. For example, Figure 16-5 illustrates the autocorrelation for an LFM chirp that is normalized so the match point is at 0 dB. Figure 16-5 shows the ideal pulse compressed response having –13 dB peak sidelobes (these may be reduced using weighting; see the section "Amplitude Weighting").

***Resolution and Range Sidelobes.*** Similar to an antenna radiation pattern, the matched filter mainlobe is the delay region immediately surrounding the matched position. Using the LFM matched filter response in Figure 16-5 as an example, it is predominantly the width of the mainlobe that determines if two closely spaced targets in range can be resolved. Therefore, if the matched filter is applied to the echoes generated by the two targets of Figure 16-2 (assuming the pulse was modulated with an LFM waveform), the pulse compressed output would look like the result shown in Figure 16-6.

As it is much shorter than the pulse width, the width of the mainlobe enables improved range resolution. The range resolution is now inversely proportional to the bandwidth of the waveform. A convenient point of reference is that a range resolution of 30 cm corresponds to a waveform bandwidth of approximately 500 MHz.

Referring again to Figure 16-5, the smaller peaks surrounding the mainlobe are known as *range sidelobes*. For the LFM chirp, the largest sidelobe is approximately 13 dB lower than the value at the matched position and defines the *peak sidelobe level* (PSL). Range sidelobes are one of the performance trade-offs of pulse compression, as they limit the sensitivity of the radar. For example, if the received power of the two target echoes depicted in Figure 16-6 were very different, the matched filter response would instead look like the result in Figure 16-7, in which the range sidelobes induced by the higher-power target can actually mask the mainlobe of the lower-power target.

***Doppler Effects and the Ambiguity Function.*** The discussion thus far has been limited to the case where no Doppler effects are present. Doppler is a shift in frequency that is induced by radial motion between the radar and the subject of the radar illumination (see Chapter 18 for a detailed discussion). For example, a police radar measures the amount of frequency shift of the echo from a moving vehicle to measure its speed relative to the position of the radar. Relative motion towards the radar causes a positive frequency shift (i.e., a higher frequency echo), while relative motion away from the radar causes a negative shift (i.e., a lower frequency echo).

With regard to pulse compression, the impact of motion-induced Doppler frequency shift is an altering of the phase progression of the waveform echo. As a result, the gain from constructive combining at the matched position (see Figure 16-3) can be degraded or even completely lost depending on the degree of Doppler shift and the nature of the waveform.

A plot of the matched filter response versus Doppler frequency shift is shown in Figure 16-8. This is defined as the *ambiguity function* (see Chapter 11).

The matched position is located where both delay and Doppler are zero. The zero Doppler cut (horizontally across Doppler = 0 Hz) reveals the waveform autocorrelation (and is the same result shown in Fig. 16-5). In the Doppler dimension the mainlobe width is inversely proportional to the pulse width. Away from the mainlobe, range-Doppler sidelobes can be observed.

In current fielded radar systems, the two most commonly employed waveforms are the LFM chirp and the biphase (or binary phase)-coded waveform. The following sections outline the benefits and deficiencies of each.

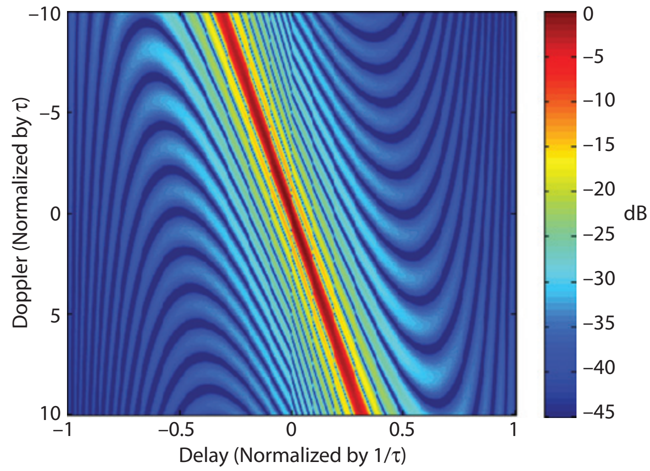


**Figure 16-8.** Delay/Doppler ambiguity function for the LFM chirp (brightness scale in decibels).

## 16.2 Linear Frequency Modulation (Chirp)

Because of its similarity to the chirping of a bird, its inventors called this form of modulation a "chirp." Since it was the first pulse compression technique, the term chirp is still in common usage and is synonymous with pulse compression.

For LFM chirp coding, the frequency of the transmitted pulse is increased (an "up-chirp") or decreased (a "down-chirp") at a constant rate throughout its length (see Figure 16-9), thus every echo has the same linear increase/decrease in frequency.

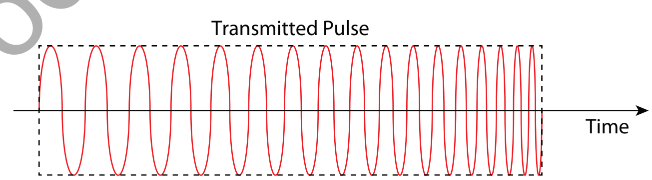


**Figure 16-9.** An LFM up-chirp.

***LFM Implementation.*** A major benefit of LFM chirp is the ease with which it can be implemented. The transmitter needs only to sweep linearly from some starting frequency at the beginning of the pulse to some ending frequency at the tail of the pulse, which can be accomplished in many different ways in both analog and digital hardware.

Filtering may be done with an analog device—such as an acoustical delay line—or, more common in modern systems, digitally. For a narrow range swath the LFM chirp can be decoded using a technique called *stretch processing*, which can accommodate a very large waveform bandwidth, thus enabling very fine range resolution.

For stretch processing (described in detail in the accompanying panel, the echo delay time (range) is converted to frequency. As a result, the return from any one range corresponds to a constant frequency, and the returns from different ranges may be separated with a bank of narrowband filters implemented with the efficient fast Fourier transform (see Chapter 21). Range is determined by measuring the instantaneous difference between the frequencies of the transmitted and received signals.

Incidentally, stretch processing is similar to the FM ranging technique used by continuous wave (CW) radars (see Chapter 17). The principal differences are that instead of transmitting pulses, the CW radar transmits continuously, and the period over which the transmitter's frequency changes in any one direction is many times the round-trip ranging time.

# Stretch Processing of LFM Chirp

For a narrow range swath, such as is mapped by a synthetic aperture radar (see Chapter 33), LFM chirp modulation is commonly decoded by a technique called *stretch processing* or *deramping*.

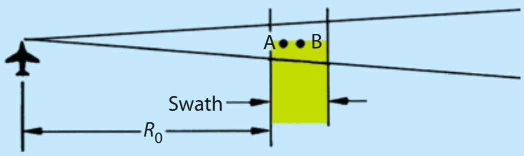


For the up-chirp example, as the return from the swath is received, its frequency is subtracted from a reference frequency that increases at the same rate as the transmitter frequency. However, the reference frequency increases continuously throughout the entire interval over which echoes are received.

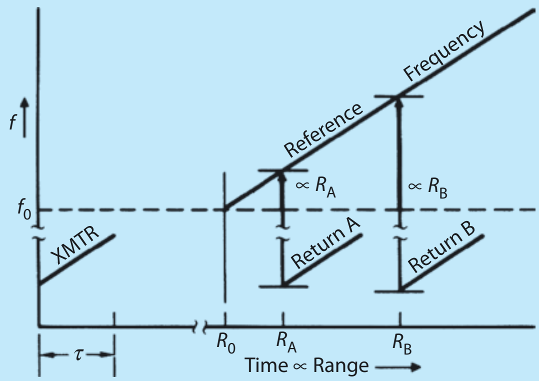


Consequently, the difference between the reference frequency and the frequency of the return from any particular point on the ground is constant. Moreover, as can be seen from the above figure, if we subtract the reference frequency's initial offset, $f_0$, from the difference already obtained, the result is proportional to the range of the point from the near edge of the swath, $R_0$. Range is thus converted to frequency.

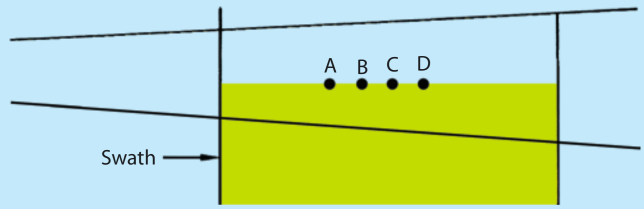


To see how fine resolution is achieved, consider the returns from four closely spaced points after the subtraction has been performed.

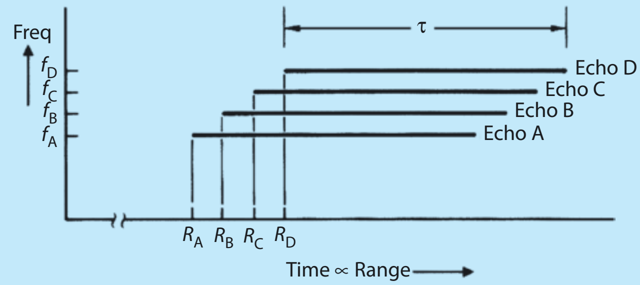


Although the returns were received such that their pulse echoes almost completely overlap, the slight stagger in their arrival times results in clearly discernible differences in frequency.

As indicated in the figure below, the continuously changing reference frequency may be subtracted at one of three points in the receiving system. One is the mixer, which converts the radar returns to the receiver's intermediate frequency (IF). The second point is the synchronous detector, which converts the output of the IF amplifier to video frequencies. And the third point is in the signal processor, after the video has been digitized.

To sort the difference frequencies, the video output of the synchronous detector is applied to a bank of narrowband filters, implemented with the fast Fourier transform.

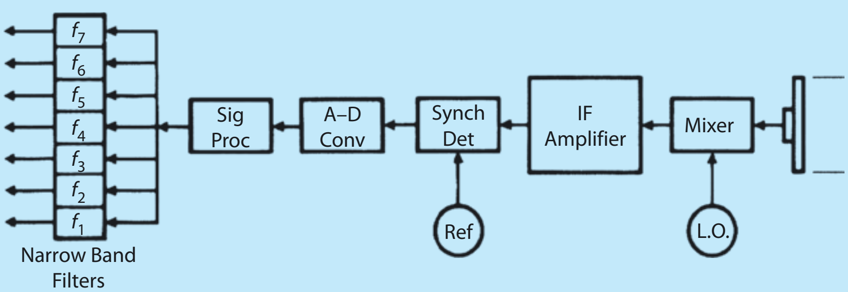


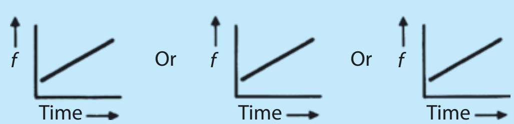

***Pulse Compression Ratio.*** The straightforward nature of the LFM provides a convenient framework with which to better explain the processing gain and range resolution enhancement provided by pulse compression. The pulse compression ratio, represented by the factor 8 for the example in Figure 16-3, is the ratio of the uncompressed pulse width $\tau$ to the compressed width $\tau_{comp}$. Whereas the previous example explained the phenomenon in terms of phase-modulated subpulses, LFM chirp allows us to consider it in terms of frequency sensitivity.

If returns received simultaneously from two slightly different ranges are to be separated on the basis of the difference in their frequencies, besides providing a delay proportional to frequency (refer to the panel on stretch processing), a second requirement must also be satisfied. The frequency difference must be large enough for the signals to be resolved by the filter.

As will be made clear in Chapter 20, the frequency resolution of the matched filter response increases (becomes narrower) as the uncompressed pulse width increases (see Figure 16-10). Specifically, the frequency resolution $\Delta f$ is related to the uncompressed pulse width as

$$\Delta f = \frac{1}{\tau}.$$

In other words, as illustrated by Figure 16-11, for the LFM matched filter to resolve two closely spaced echoes, the instantaneous difference in their delay-shifted frequencies must meet or exceed the inverse of the uncompressed pulse width $\tau$.

Furthermore, the compressed pulse width $\tau_{comp}$ is the period of time over which the frequency of the uncompressed LFM pulse changes by $\Delta f$ (see Figure 16-12). By extension, if the frequency of the uncompressed LFM pulse changes at a rate of $\Delta f/\tau_{comp}$ (in hertz per second), then the total change in frequency, $\Delta F$, over

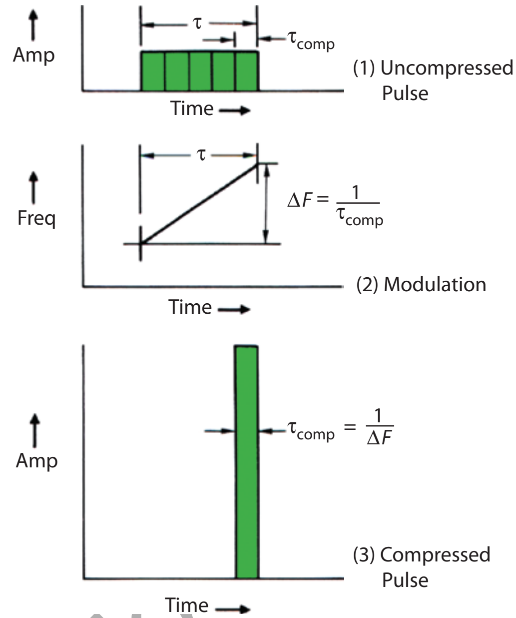


**Figure 16-10.** Conceptual relationship between uncompressed pulse width, chirp modulation bandwidth $\Delta F$, and compressed pulse width for an LFM waveform. The compressed pulse width corresponds to the mainlobe from Figure 16-5.

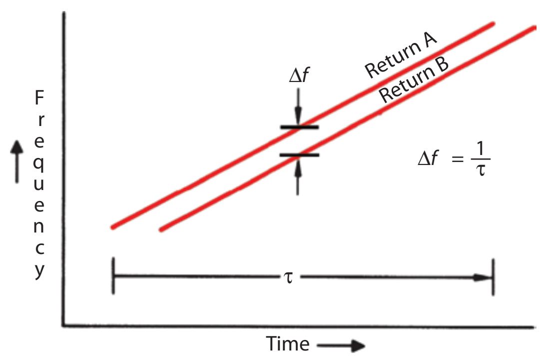


**Figure 16-11.** For a filter to resolve two concurrently received LFM returns, the instantaneous difference in their frequencies ($\Delta f$) must equal at least $1/\tau$.

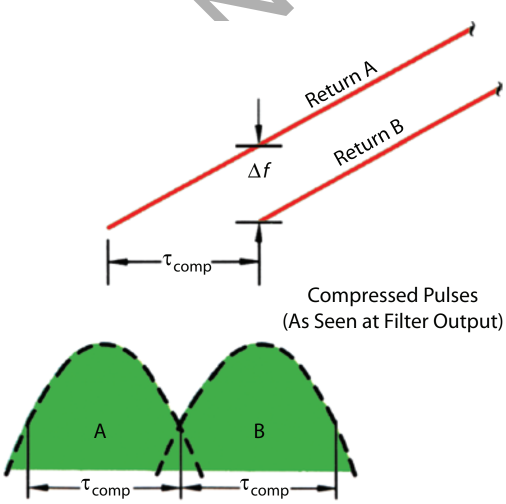


**Figure 16-12.** If the minimum resolvable frequency difference is $\Delta f$, the time in which the frequency of the uncompressed LFM pulse changes by $\Delta f$ is the width of the compressed pulse, $\tau_{comp}$.

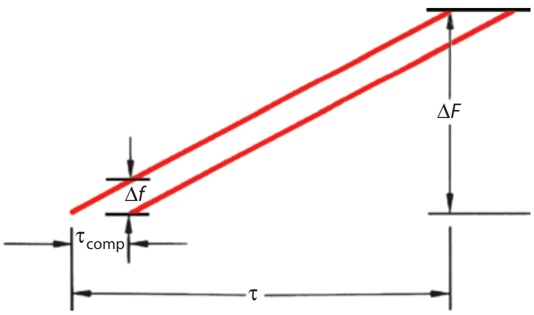


**Figure 16-13.** The ratio of uncompressed pulse width, $\tau$, to compressed pulse width, $\tau_{comp}$, equals the ratio of the total change in frequency over the pulse width, $\Delta F$, to minimum resolvable frequency difference, $\Delta f$.

the duration of the uncompressed pulse will be this rate times the uncompressed pulse width, $\tau$.

The rate of frequency change $\Delta f/\tau_{comp}$ is known as the *chirp rate*:

$$\text{chirp rate} = \frac{\Delta f}{\tau_{comp}} \text{ (in hertz per second).}$$

The total change in frequency, $\Delta F$, is the *bandwidth* for the LFM chirp:

$$\text{bandwidth} = \Delta F = \left(\frac{\Delta f}{\tau_{comp}}\right)\tau = \text{chirp rate} \times \tau.$$

As is apparent from the geometry of Figure 16-13, the pulse compression ratio, $\tau/\tau_{comp}$, equals the ratio of $\Delta F$ to $\Delta f$:

$$\text{Pulse compression ratio} = \frac{\tau}{\tau_{comp}} = \frac{\Delta F}{\Delta f}.$$

Substituting $1/\tau$ for $\Delta f$, the pulse compression ratio equals the uncompressed pulse width times $\Delta F$:

$$\text{Pulse compression ratio} = \tau\Delta F.$$

The quantity $\tau\Delta F$ is also called the *time–bandwidth product*.

This simple relationship—pulse compression ratio equals time–bandwidth product—tells us a lot about the LFM chirp. To begin with, for a given uncompressed pulse width $\tau$, the compression ratio increases directly with an increase in bandwidth $\Delta F$. Conversely, for a given bandwidth $\Delta F$, the compression ratio increases directly with an increase in the uncompressed pulse width $\tau$.

If the time–bandwidth product is set equal to $\tau/\tau_{comp}$ as

$$\tau\Delta F = \frac{\tau}{\tau_{comp}},$$

$\tau$ cancels out so that

$$\tau_{comp} = \frac{1}{\Delta F}.$$

In other words, the width of the compressed pulse is determined entirely by the bandwidth $\Delta F$ of the transmitted pulse; that is, the greater the frequency change, the narrower the compressed pulse width. Rearranging this last equation tells us that the total change in transmitter frequency (the LFM bandwidth) must be

$$\Delta F = \frac{1}{\tau_{comp}}.$$

This relationship provides a useful benchmark for the transmitter bandwidth necessary to achieve a desired bandwidth (and therefore range resolution) for arbitrary waveforms. It should be noted, however, that the equality only holds for the LFM chirp, which spends an equal amount of time (and thus power) in each of the frequencies due to its linear frequency sweep. Different waveforms that occupy some frequencies longer than others or employ a weighting across frequencies may require a higher bandwidth to achieve the same compressed pulse width as the LFM.

To get a feel for the relative values involved for LFM chirp, consider a couple of representative examples.

- Using LFM to provide the same compression as in the 8-chip matched filter discussed earlier, $\tau/\tau_{comp} = 8$. If the original pulse is 1 μs, the range resolution has now improved to 18.75 m. This would separate aircraft targets except for very tight formations of small planes.
- It is assumed that in order to provide adequate "energy on target," the width of a radar's transmitted pulse must be $\tau = 10$ μs. To provide the desired range resolution of 1.5 m, a compressed pulse width of $\tau_{comp} = 0.01$ μs is required. Therefore the pulse compression ratio must be

$$\frac{\tau}{\tau_{comp}} = \frac{10}{0.01} = 1000$$

To achieve a compressed pulse width of 0.01 μs ($10^{-8}$ s), the change in transmitter frequency, $\Delta F$, over the duration of each transmitted pulse must be $1/10^{-8} = 10^8$ Hz, or a bandwidth of 100 MHz.

Since the duration of the uncompressed pulse is 10 μs ($10^{-5}$ s), the rate of change of the transmitter frequency (the chirp rate) will be $10^8/10^{-5} = 10^{13}$ Hz/s, or 10,000 GHz/s. This arrangement equates to a total linear frequency modulation excursion of 100 MHz over the duration of the pulsed waveform.

Incidentally, these values explain why stretch processing is practical only for relatively narrow range intervals. The ranging time for an interval of 100 km, for instance, is $13.3 \times 50 = 665$ μs. If the receiver local-oscillator frequency is shifted at a rate of 10 GHz/s throughout that time (see Figure 16-14), the total frequency shift would be $10{,}000 \times 620 \times 10^{-6} = 6.65$ GHz. Such a large shift was deemed impractical in previous editions of this book and is only now beginning to enter the realm of possibility.



***LFM Ambiguity Function.*** LFM allows very large compression ratios to be achieved with a relatively simple implementation. To assess the performance capability of LFM, consider its delay and Doppler characteristics that were illustrated via the ambiguity function in Figures 16-5 and 16-8.

One disadvantage of LFM is the high sidelobes that occur in the range dimension. These high sidelobes have driven the development of alternative waveforms and filtering strategies.

Another possible disadvantage is the ambiguity that occurs between range and Doppler (the range–Doppler ridge), shown in Figure 16-8. If an echo possesses a sufficient Doppler shift, it will also appear to be shifted in range, thereby limiting the ultimate accuracy for which true range may be determined. However, this *Doppler tolerance* also allows for simpler receiver

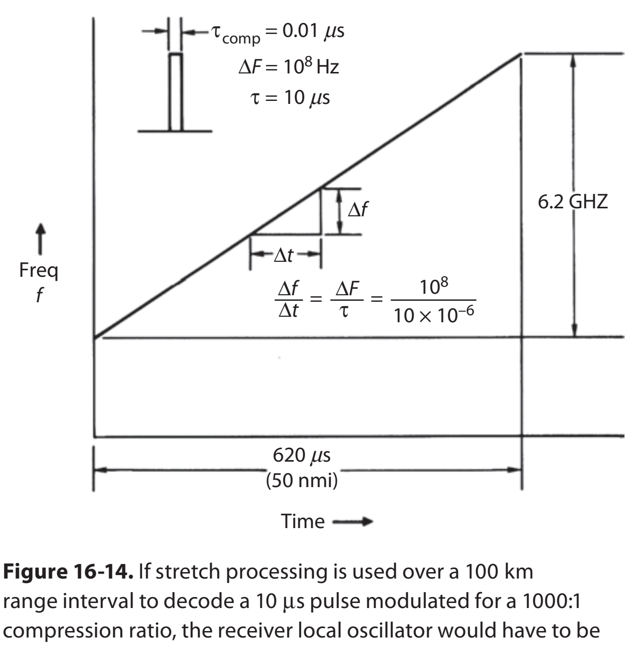


**Figure 16-14.** If stretch processing is used over a 100 km range interval to decode a 10 μs pulse modulated for a 1000:1 compression ratio, the receiver local oscillator would have to be swept over 6.65 GHz.

processing by precluding the need for a bank of matched filters tuned to different possible Doppler frequencies.

***Amplitude Weighting.*** A well-known approach to reduce range sidelobes for LFM is to apply an amplitude weighting to the waveform that reduces the power in the regions nearer the ends of the pulse. Due to the frequency-swept nature of LFM, this weighting results in a deemphasizing of the frequencies near the extremities of the bandwidth, which results in lower sidelobes in the time domain due to the relationship between time and frequency (from Chapter 6).

The trade-off for this significant reduction in range sidelobes is reduced transmit power, which directly impacts detection sensitivity. This weighting can also cause a degradation in range resolution due to reduced power in the outer frequencies, which is essentially a reduction in bandwidth. A typical compromise is to allow the resolution size to increase by approximately 50%, which enables sidelobe levels to be around –35 to –40 dB or less.

From an implementation standpoint, weighting the transmitted pulse may also be prohibitive if high-efficiency, nonlinear amplification is required.

A common compromise is to transmit the standard LFM waveform while applying a receive filter that is weighted. This form of *mismatched filtering* has the advantage of still enabling the maximum power on transmit as well as power-efficient nonlinear amplification. The trade-off is a small mismatch loss between the waveform and filter that is acceptable for many radar applications.



## 16.3 Phase Modulation

In this type of coding the waveform is represented as a discrete sequence of increments, with each increment corresponding to one from a set of phase values modulated onto a *subpulse* (or *chip*). The set of possible phase values is often referred to as the phase *constellation*. For practical reasons, it is often desirable for the nature of the subpulse shape to provide continuous transitions between adjacent subpulses.

***Binary Phase Modulation.*** The simplest form of phase modulation employs a constellation of two opposite phase values (usually 0° and 180°) that are modulated onto a subpulse. The radio frequency phase of certain subpulse segments is shifted by 180° (or –1), according to a predetermined binary code. The subpulse is comprised of a multiple number of wavelengths of the carrier frequency.

Figure 16-15 illustrates an exemplary three-segment code. (So you can readily discern the phases, the wavelength has been arbitrarily increased to the point where each segment contains only one cycle.)

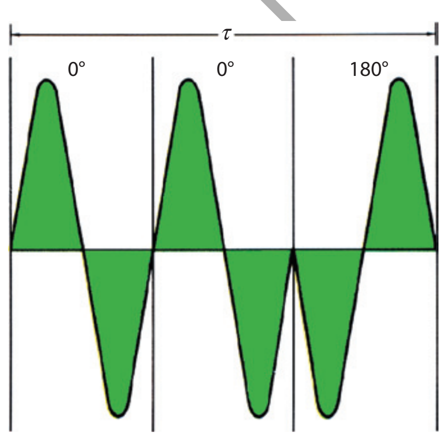


**Figure 16-15.** Binary phase coding of a transmitted pulse. The pulse is marked off into segments and the phases of certain segments (here, the third) are reversed.

A common shorthand method of indicating the coding is to represent the segments with + and – signs. An unshifted segment (0°) is represented by a + sign and a shifted segment (180°) by a – sign. The signs making up the code are referred to as digits. The number of digits indicates the pulse compression ratio of the code.

The received echoes are passed through a tapped delay line (Figure 16-16) that provides a time delay exactly equal to the duration of the uncompressed pulse, $\tau$. The delay line may be implemented either with an analog device or digitally. Clearly the tapped delay line for the binary-coded waveform is an implementation of the matched filter previously shown in Figures 16-3 and 16-4.

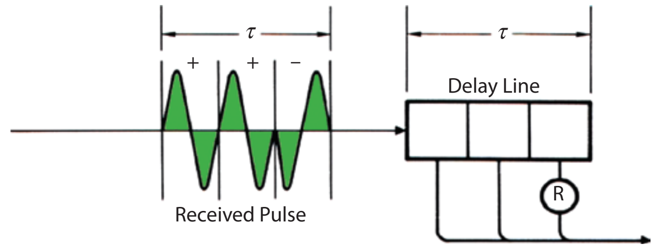


**Figure 16-16.** Received pulse echoes are passed through a tapped delay line filter. A separate tap is provided for each segment of the pulse. Here, the third tap is reversed R to represent a 180° phase shift.

Like the transmitted pulse, the delay line is divided into segments. An output tap is provided for each segment. The taps are all tied to a single output terminal. At any instant, the signal at the output terminal corresponds to the sum of whatever segments of a received pulse currently occupy the individual segments of the line.

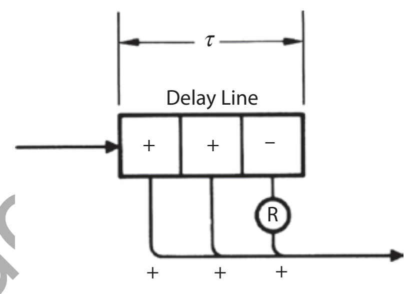


**Figure 16-17.** The phase reversal ® is placed so that when a pulse completely fills the delay line, outputs from all taps will be in phase.

Now, in certain taps, 180° phase reversals are inserted. Their positions correspond to the positions of the phase-shifted segments in the transmitted pulse. Thus when a received echo has progressed to the point where it completely fills the line, the outputs from all of the taps will be in phase (Figure 16-17). Their sum will then equal the amplitude of the pulse times the number of segments it contains.



To see step by step how the binary-coded pulse is compressed, consider a simple three-segment delay line and the three-digit code, illustrated in Figure 16-15.

Suppose the echo from a single-point target is received. Initially the output from the delay line is zero. When segment 1 of the echo has entered the line, the signal at the output terminal corresponds to the amplitude of this segment (Figure 16-18). Since its phase is 180°, the output is negative: –1.

An instant later, segment 2 has entered the line. Now the output signal equals the sum of segments 1 and 2. Since the segments are 180° out of phase, however, they cancel: the output is 0.

When segment 3 has entered the line, the output signal is the sum of all three segments. At this point segment 1 has reached the tap containing the phase reversal. The output from this tap is, therefore, in phase with the unshifted segments 2 and 3 such that the combined output of the three taps is three times the amplitude of the individual segments: +3.

As segments 2 and 3 pass through the line, this process continues. The output drops to 0, then becomes –1, and finally returns to 0 again.

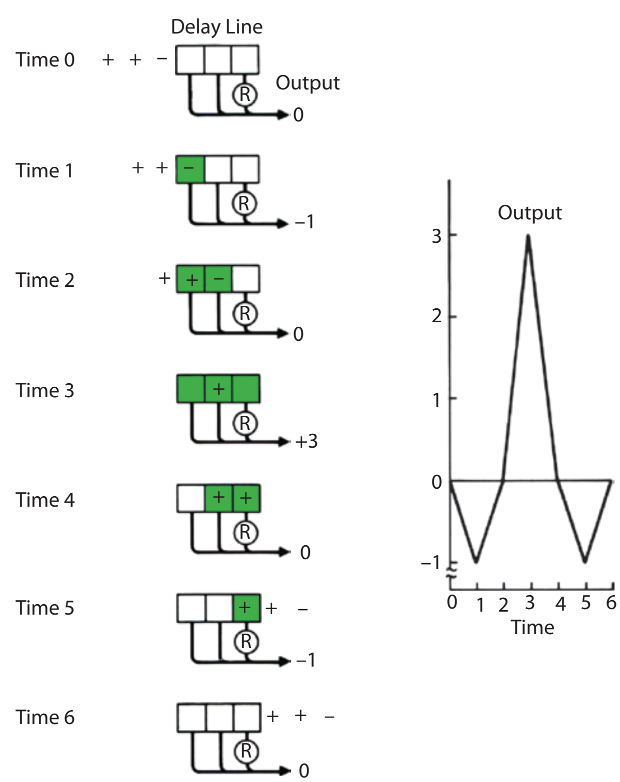


**Figure 16-18.** Step-by-step progress of a three-digit binary phase modulated pulse through a tapped delay line.

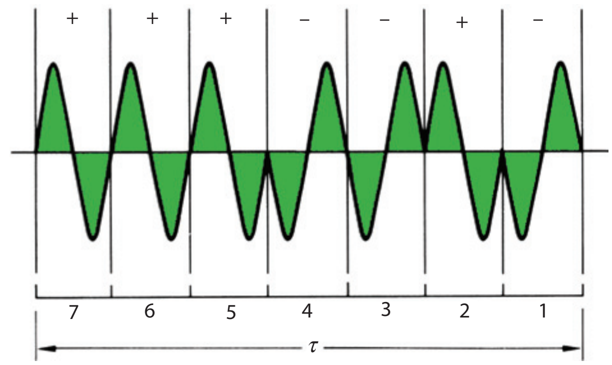


**Figure 16-19.** A seven-digit binary phase code.

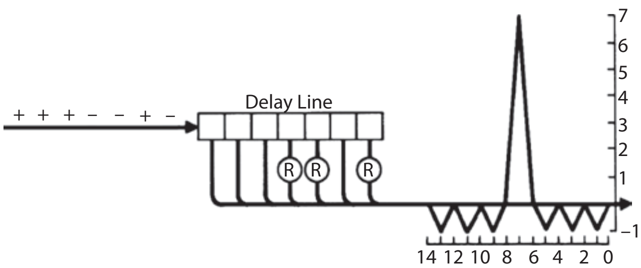


**Figure 16-20.** Output produced when a seven-digit binary phase code is passed through a tapped delay line with phase reversals in the appropriate taps.

| N | Barker Codes |
|---|---|
| 2 | + − Or (+ +) |
| 3 | + + − |
| 4 | + − + − Or (+ − − −) |
| 5 | + + + − + |
| 7 | + + + − − + − |
| 11 | + + + − − − + − − + − |
| 13 | + + + + + − − + + − + − + |

Note: Plus and minus signs may be interchanged
(+ + − changed to − − +); order of digits may be reversed
(+ + − changed to − + +). Codes in parentheses are complementary codes.

**Figure 16-21.** Barker codes come very close to the goal of producing no sidelobes. However, the largest Barker code contains only 13 digits.

A somewhat more practical example is shown in Figure 16-19. This code has seven digits. Assuming no losses, the peak amplitude of the compressed pulse is seven times that of the uncompressed pulse, and the compressed pulse is only one-seventh as wide.

To see why the code produces the output it does, transfer the code to a sheet of paper and slide it across the delay line plotted in Figure 16-20, digit by digit, noting the sum of the outputs for each position. (A minus sign, –, over a tap with a reversal ® in it becomes a +, while conversely the reversal of a + becomes a –.) You should obtain the output shown in the figure.

***Barker Codes.*** Ideally, for all positions of the echo in the line—except the central one—the collection of 0° or 180° outputs would cancel and there would be no range sidelobes.

One set of codes, called the Barker codes, comes very close to meeting this goal (Figure 16-21). Two of these codes have been used in the above examples. As has been seen, they produce sidelobes whose amplitudes are no greater than the amplitude of the individual code segments. Consequently the ratio of mainlobe amplitude to sidelobe amplitude, as well as the pulse compression ratio, increases with the number of segments into which the pulses are divided—that is, the number of digits in the binary code.

Unfortunately, the longest Barker code contains only 13 digits. Arbitrary binary codes can be made practically any length, but their sidelobe characteristics, though reasonably good, do not possess this desirable property of the Barker codes. Such codes require an exhaustive computer search and are called *minimum peak sidelobe* codes.

***Complementary Codes.*** It turns out that the four-digit Barker code has a special feature that enables us to build codes of greater length and even eliminate the sidelobes altogether (under certain conditions). This feature arises because the four-digit code, as well as the two-digit code, has a complementary form. The sidelobe structures produced by the complementary forms have opposite phases (Figure 16-22). Therefore, if successive transmitted pulses are alternately modulated with the two forms of the code and filter each with their corresponding delay line, the returns from successive pulses can be added such that the sidelobes cancel.

Furthermore, by chaining the complementary forms together according to a certain pattern, codes of much greater length can be built. As illustrated in Figure 16-23, the two forms of the four-digit code are just such combinations of the two forms of the two-digit code, and these are just such combinations of the two fundamental binary digits, + and –.

Unlike the unchained Barker codes, the chained codes (also called *nested codes*) produce sidelobes having amplitudes greater than one. However, since the chains are complementary, these larger sidelobes—like the others—cancel when successive pulses are added (at least in the absence of Doppler).

***Doppler Sensitivity.*** Compared with LFM chirp, coded modulations can be much more sensitive to Doppler frequency shift. If all segments of a phase-coded pulse are to add constructively when the pulse is centered in the delay line, while cancelling when it is not, very little additional shift in phase over the length of the pulse can be tolerated.

A Doppler shift of 10 kHz amounts to a phase shift of 10,000 × 360°/s, or 3.6°/μs. If the uncompressed pulse width is as much as 50 μs (Figure 16-24), this shift will itself equal 180° over the length of the pulse, and performance will deteriorate. For the scheme to be effective, either the Doppler shifts must be comparatively small or the uncompressed pulses must be reasonably short.

One way to contend with phase-coding sensitivity to Doppler is through "Doppler tuning," in which a bank of Doppler-shifted versions of the delay line matched filter outputs are applied. While this approach increases the overall hardware (analog filtering) or computational (digital filtering) requirements, it does have the benefit of avoiding the range–Doppler ambiguity problem of the LFM chirp.

The sidelobe cancellation property of complementary code sets is very sensitive to pulse-to-pulse Doppler shift. The sidelobes do not perfectly subtract when Doppler is present, so residual sidelobes emerge.

***Polyphase Codes.*** Phase coding is not limited to just two increments (0° and 180°). Codes with phase constellations comprised of more than two possible values are collectively referred to as *polyphase codes*. Here a particular example is considered and is taken from a family called Frank codes.

The fundamental phase increment ϕ for a Frank code is established by dividing 360° by the number of different phases in the constellation, *P*. The coded pulse is then built by chaining together *P* groups of *P* segments each. The total number of segments in a pulse, therefore, equals $P^2$.

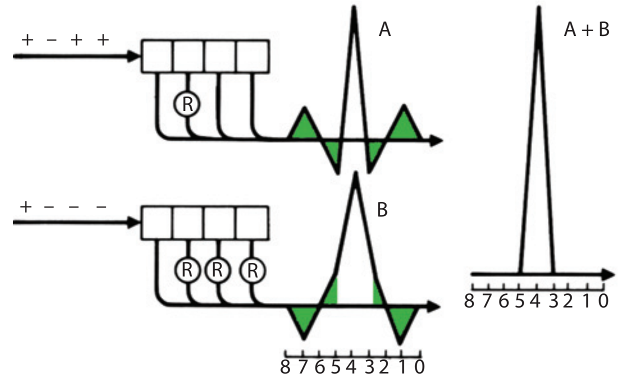


**Figure 16-22.** Echoes from complementary phase coding received from the same target in alternating pulses. When echoes are added, the time sidelobes cancel.

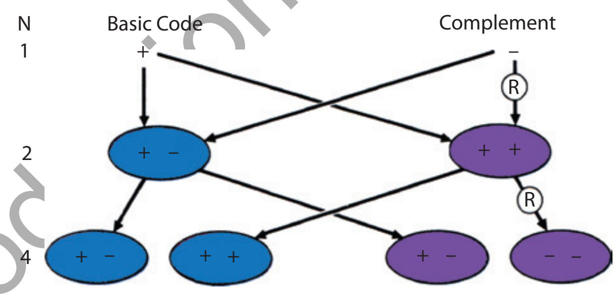


**Figure 16-23.** How complementary codes are formed. The basic two-digit code is formed by chaining a basic binary digit (+) to its complement (–). A complementary two-digit code is formed by chaining a basic binary digit (+) to its complement with the sign reversed (+). The basic four-digit code is formed by chaining a basic two-digit code (+ –) to its complementary two-digit code (+ +). A complementary four-digit code is formed by chaining a basic two-digit code (+ –) to its complementary two-digit code with the sign reversed (– –), and so on.

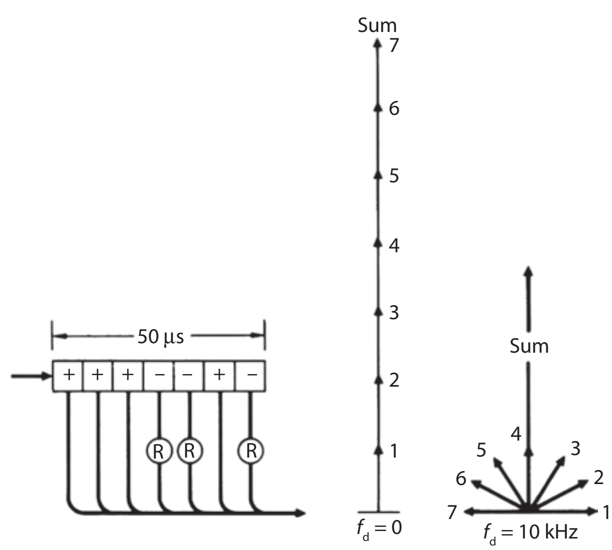


**Figure 16-24.** The reduction in peak output of a tapped delay line for a 50 μs, phase-coded pulse resulting from a Doppler shift of 10 kHz.

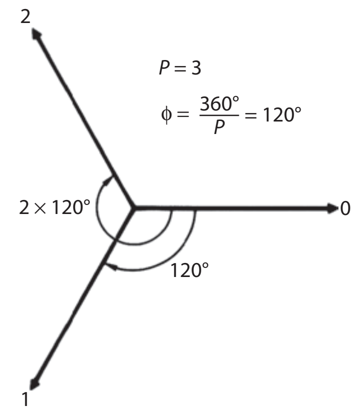


**Figure 16-25.** Phase increments for a Frank code in which the number of phases *P* is three.

In a three-phase code (Figure 16-25), for example, the fundamental phase increment is $360° \div 3 = 120°$, making the phases 0°, 120°, and 240°. The coded pulse consists of three groups of three segments—a total of nine segments.

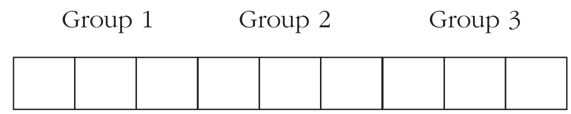


Phases are assigned to the individual segments according to two simple rules: (1) the phase of the first segment of every group is 0°, that is, 0° ___ ___, 0° ___ ___, 0° ___,___; and (2) the phases of the remaining segments in each group increase in increments of

$$\Delta\Phi = (G - 1) \times (P - 1) \times \phi°,$$

where

$G$ = group number

$P$ = number of phases

$\phi$ = basic phase increment.

For a three-phase code ($P = 3$, $\phi = 120°$, $P - 1 = 2$), then $\Delta\Phi = (G - 1) \times 2\phi$. So the phase increment in Group 1 is 0°, the phase increment for Group 2 is $2\phi$, and the phase increment for Group 3 is $4\phi$.

Written in terms of $\phi$, the nine digits of the code for $P = 3$ are

| Group 1 | Group 2 | Group 3 |
|---|---|---|
| 0, 0, 0 | 0, $2\phi$, $4\phi$ | 0, $4\phi$, $8\phi$ |

Substituting 120° for $\phi$ and dropping multiples of 360°, the code becomes

| Group 1 | Group 2 | Group 3 |
|---|---|---|
| 0°, 0°, 0° | 0°, 240°, 120° | 0°, 120°, 240° |

Echoes are decoded by passing them through a tapped delay line (or the digital equivalent) in the same way as binary phase-coded echoes (Figure 16-26). The only difference is, the phase shifts in the taps have more than one value.

For a given number of segments, a Frank code provides the same pulse compression ratio as a binary phase code and the same ratio of peak amplitude to sidelobe amplitude as a Barker code. Yet, by using more phases (increasing *P*), the codes can be made of the greater length, $P^2$. As *P* is increased, however, the size of the fundamental phase increment decreases, making performance more sensitive to externally introduced phase shifts (e.g., transmitter distortion) and imposing more severe restrictions on uncompressed pulse width and maximum Doppler shift.

Frank codes are an example of a class of codes in which the discrete phase sequence can be viewed as a sampled version of the LFM chirp. Other such codes are the Zadoff-Chu code, the "P" codes, and Golomb codes. Like the minimum peak

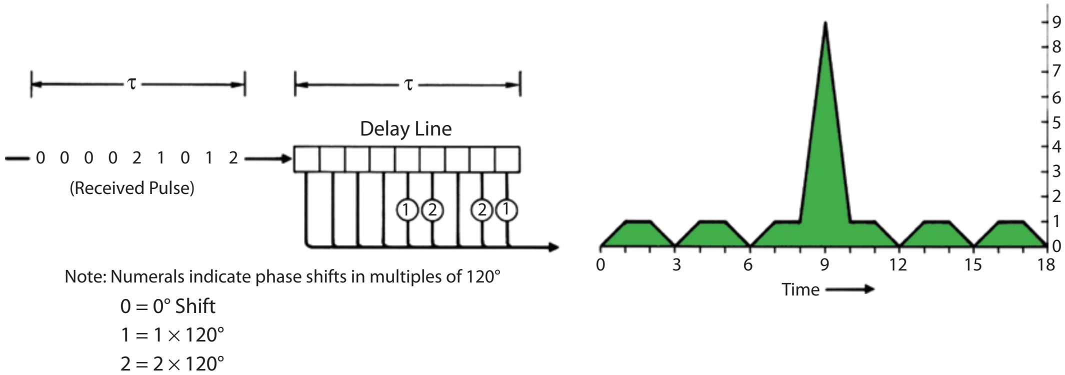


**Figure 16-26.** Processing of Frank codes is similar to that of binary codes. Phase shifts introduced in taps complement shifts in corresponding segments of the coded pulse. If the phase of a segment is shifted by 1 × 120°, the corresponding tap adds a shift of 2 × 120°, making the total shift when the pulse fills the line equal 3 × 120° = 360°. This phase relationship is identical to the matched filter.

sidelobe codes for the binary phase constellation, it is also possible to perform an exhaustive computer search for polyphase codes of arbitrary length and phase constellation.

While binary codes are in widespread use, the implementation of polyphase codes is more limited. The reason is that binary codes can be implemented in a phase-continuous manner in the transmitter while, until very recently, polyphase codes could not. These phase discontinuities at the chip transitions produce spectral spreading and can also limit the fidelity with which a polyphase-coded waveform can be generated by a practical transmitter. However, the design freedom provided by polyphase codes serves as the basis for new emerging radar capabilities. This topic is discussed further in Chapter 45.



## 16.4 Summary

Since radar transmitters are peak power limited, pulse compression provides the means to achieve sufficient energy on target for detection while enabling the requisite range resolution. Pulse compression comprises transmission of a modulated waveform and receiver filtering to compress the resulting echoes in range.

The most commonly used pulse compression techniques are the LFM chirp and binary phase coding.

With LFM, the frequency of each transmitted pulse is continuously increased or decreased. Applying the receive filter that is matched to the waveform results in a compressed pulse width of $1/\Delta F$, where $\Delta F$ is the total change in frequency (i.e., the bandwidth) of the waveform. The LFM range sidelobes may be reduced by amplitude weighting the receiver matched filter at a cost of reduced range resolution and mismatch loss.

When only a narrow range swath is of interest, the LFM chirp can be decoded using stretch processing, whereby range is converted to frequency in the receiver. Differences in frequency are resolved by a bank of tuned filters implemented with the efficient fast Fourier transform. With the LFM waveform and stretch processing, very large compression ratios and fine range resolution can be achieved. The LFM is rather insensitive to Doppler frequency shift, though such a shift produces an ambiguity in range.

In binary phase modulation, each pulse is marked off into segments, with the phase of certain segments reversed. Received echoes are passed through a tapped delay line having phase reversals in taps corresponding to those in the code. Binary codes are more sensitive to Doppler frequency shift than the LFM chirp.

Barker codes represent a form of binary phase modulation in which the mainlobe-to-sidelobe ratio equals the pulse–compression ratio, though the longest Barker code is only 13 digits.

Sidelobes may be eliminated by alternately transmitting complementary codes that are obtained from chained Barker codes. However, this property requires little to no Doppler shift.

Polyphase (e.g., Frank) codes can also be used, but these are more sensitive to Doppler shift than binary codes, due to smaller phase increments. Polyphase codes tend to produce phase discontinuities, which results in spectral spreading and sensitivity to transmitter distortion.



## Further Reading

1. N. Levanon and E. Mozeson, *Radar Signals*, John Wiley & Sons, 2004.
2. M. A. Richards, J. A. Scheer, and W. A. Holm, eds., *Principles of Modern Radar: Basic Principles*, SciTech, 2010, chap. 20.

## Test your understanding

1. To achieve a range resolution of 0.5 m with a 20 μs pulse, determine the required chirp rate and the associated pulse compression ratio.
2. Using the process described in Figure 16-18, determine the tapped delay line output for the following binary codes:
   a. Length 11 Barker code as defined in Figure 16-21
   b. [+ + + − − − + − − + +] (Barker 11, but with the last digit flipped)
3. Using the tapped delay line outputs from problem 2, determine the largest sidelobe value relative to the mainlobe. This ratio is known as the PSL.
4. For $P = 4$ phase values, determine the length 16 Frank code and compute its output from the tapped delay line.

STIMSON'S

# Introduction to Airborne Radar

## Third Edition

Completely modernized, greatly expanded, but retaining all the magic of the 2nd edition, *Introduction to Airborne Radar* has been brought into the 21st century without losing the hallmarks that made George Stimson's previous editions unique. Every chapter has been updated to reflect the constant transformations in radar technology and end-of-chapter exercises have also been added, improving its employment as a textbook.

Over 100 radar and EW experts from around the world were involved in reviewing, writing, and editing this book, each one a longtime user of the previous editions. Each one of them was tasked with making sure this third edition lives up to its legacy of "Introduction."

*Stimson's* is written specifically as an overview without going overboard on the math. Virtually anyone with a knowledge of high school algebra, trigonometry, and physics will be able to read and absorb the vast majority of the material. The first 17 chapters provide fundamentals that can be used by air, ground, and sea-based personnel. Every chapter provides extensive fundamental materials and practical applications, using visual system exemplars to aid explanations. The unique full color layout is enhanced with an immense number of illustrations, figures, tables, and color photographs.

### KEY FEATURES

- Modernized to reflect changes in the past 20 years including electronic scanning antennas and high resolution imaging.
- Completely covers the wide range of techniques employed in modern airborne and space borne radars.
- Fundamentals are applicable to ground and sea-based radar.
- Clear, understandable writing supplemented by extensive graphic illustration of concepts and offset boxes taking those concepts to the next level.
- Community reviewed by over 100 radar experts from organizations worldwide.

### AUDIENCE

- Military pilots, radar intercept officers, ground crews, and avionics technicians.
- Radar engineers/technicians.
- Students (academic and industry training) in radar, aviation, and aeronautics (end-of-chapter exercises now included).
- Radar and electronic warfare marketing and sales personnel.

### ABOUT THE EDITORS

**Hugh D. Griffiths** is the Thales/Royal Academy of Engineering Chair of RF Sensors within the Department of Electronic and Electrical Engineering at University College London. He has received numerous awards and serves on the IEEE AESS Board of Governors, on the IEEE AESS Radar Systems Panel, and is Editor-in-Chief of the IET Journal "IET Radar, Sonar and Navigation."

**Chris J. Baker** is the Ohio Research Scholar in Integrated Sensor Systems at The Ohio State University. Until June 2011 he was the Dean and Director of the College of Engineering and Computer Science at the Australian National University. He has been actively engaged in radar system research since 1984.

**Dave Adamy** is an internationally recognized expert in electronic warfare with 47 years experience as a systems engineer. He has published over 180 articles, has 11 books in print and is a past National President of the Association of Old Crows. For the past 26 years he has run his own company performing studies for the United States Government and defense contractors as well as teaching EW courses worldwide.

SciTech Publishing
an imprint of the IET
Edison, New Jersey
www.theiet.org